Centrifugal Instability: Taylor Vortices

Experiments indicate initially instability appears as axisymmetric disturbance such that $\frac{\partial}{\partial\theta} = 0$.

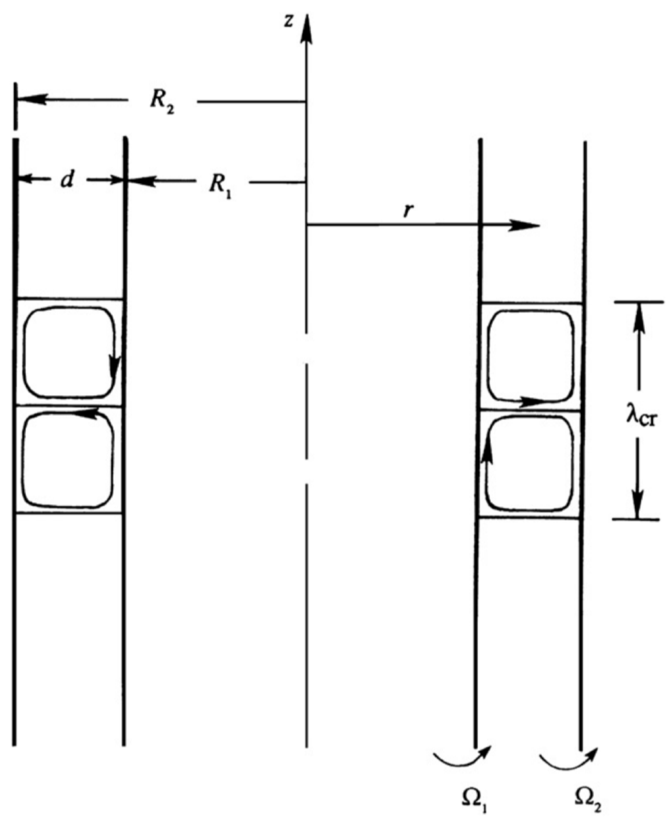

FIGURE 11.16 Geometry of the flow and the instability in rotating Couette flow. The fluid resides between rotating cylinders with radii R_1 and R_2. As for Bénard convection, the resulting instability forms as counter-rotating rolls with a wavelength that is approximately twice the gap between the cylinders.

Taylor Solution Viscous Flow

Axisymmetric (r, θ, z) equations: $\frac{\partial}{\partial\theta} = 0$

$\mathbf{V} = v_r\hat{\mathbf{e}}_r + v_\theta\hat{\mathbf{e}}_\theta + v_z\hat{\mathbf{e}}_z$

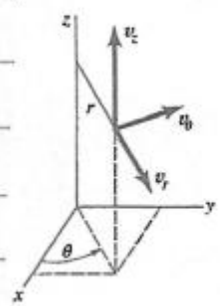

(*r* direction)

$$\rho\left(\frac{\partial v_r}{\partial t} + v_r\frac{\partial v_r}{\partial r} + \cancel{\frac{v_\theta}{r}\frac{\partial v_r}{\partial\theta}} - \frac{v_\theta^2}{r} + v_z\frac{\partial v_r}{\partial z}\right) = -\frac{\partial p}{\partial r} + \cancel{\rho g_r} + \mu\left[\frac{1}{r}\frac{\partial}{\partial r}\left(r\frac{\partial v_r}{\partial r}\right) - \frac{v_r}{r^2} + \cancel{\frac{1}{r^2}\frac{\partial^2 v_r}{\partial\theta^2}} - \cancel{\frac{2}{r^2}\frac{\partial v_\theta}{\partial\theta}} + \frac{\partial^2 v_r}{\partial z^2}\right]$$

(*θ* direction)

$$\rho\left(\frac{\partial v_\theta}{\partial t} + v_r\frac{\partial v_\theta}{\partial r} + \cancel{\frac{v_\theta}{r}\frac{\partial v_\theta}{\partial\theta}} + \frac{v_r v_\theta}{r} + v_z\frac{\partial v_\theta}{\partial z}\right) = -\cancel{\frac{1}{r}\frac{\partial p}{\partial\theta}} + \cancel{\rho g_\theta} + \mu\left[\frac{1}{r}\frac{\partial}{\partial r}\left(r\frac{\partial v_\theta}{\partial r}\right) - \frac{v_\theta}{r^2} + \cancel{\frac{1}{r^2}\frac{\partial^2 v_\theta}{\partial\theta^2}} + \cancel{\frac{2}{r^2}\frac{\partial v_r}{\partial\theta}} + \frac{\partial^2 v_\theta}{\partial z^2}\right]$$

(*z* direction)

$$\rho\left(\frac{\partial v_z}{\partial t} + v_r\frac{\partial v_z}{\partial r} + \cancel{\frac{v_\theta}{r}\frac{\partial v_z}{\partial\theta}} + v_z\frac{\partial v_z}{\partial z}\right) = -\frac{\partial p}{\partial z} + \cancel{\rho g_z} + \mu\left[\frac{1}{r}\frac{\partial}{\partial r}\left(r\frac{\partial v_z}{\partial r}\right) + \cancel{\frac{1}{r^2}\frac{\partial^2 v_z}{\partial\theta^2}} + \frac{\partial^2 v_z}{\partial z^2}\right]$$

$$\frac{1}{r}\frac{\partial(rv_r)}{\partial r} + \cancel{\frac{1}{r}\frac{\partial v_\theta}{\partial\theta}} + \frac{\partial v_z}{\partial z} = 0$$

Decompose motion into basic solution plus perturbation

$\underline{\tilde{u}} = \underline{U} + \underline{u} \qquad \tilde{p} = P + p$

Basic Solution:

$U_r = U_z = 0$

$$U_\theta = V(r) = Ar + \frac{B}{r}$$

$$\frac{\partial P}{\partial r} = \rho\frac{V^2}{r}$$

Basic solution already has already given and discussed. Perturbation equations obtained by substituting motion decomposition into axisymmetric (r, θ, z) equations, neglecting nonlinear terms, and subtracting the basic solution.

$$u_{r_t} - \frac{2V}{r} u_\theta = -\frac{p_r}{\rho} + \nu\left(\nabla^2 u_r - \frac{u_r}{r^2}\right)$$

$$u_{\theta_t} + \left(V_r + \frac{V}{r}\right) u_r = \nu\left(\nabla^2 u_\theta - \frac{u_\theta}{r^2}\right)$$

$$u_{z_t} = -\frac{p_z}{\rho} + \nu \nabla^2 u_z$$

$$u_{r_r} + \frac{u_r}{r} + u_{z_z} = 0 \quad \nabla^2 = \frac{\partial^2}{\partial r^2} + \frac{1}{r}\frac{\partial}{\partial r} + \frac{\partial^2}{\partial z^2}$$

Since the coefficients only $f(r)$, the solutions depend on exp z and t ∴ assume normal mode solutions

$$(\underline{u}, p) = (\underline{\hat{u}}, \hat{p}) e^{ikz + \sigma t}$$

$$z \to \pm\infty, \quad (\underline{\hat{u}}, \hat{p}) \text{ bounded} \Rightarrow k = \text{real}$$

Substituting normal mode solutions into perturbation equations and eliminating $\widehat{u_z}$ and $\hat{p}$ results in equations for $\widehat{u_r}$ and $\widehat{u_\theta}$, which are solved assuming narrow gap, as per Appendix A.

$$d = r_2 - r_1 \ll \frac{(r_1 + r_2)}{2}$$

$$(D^2 - k^2 - \sigma)(D^2 - k^2)\widehat{u_r} = (1 + \alpha x)\widehat{u_\theta}$$

$$(D^2 - k^2 - \sigma)\widehat{u_\theta} = -Ta\, k^2 \widehat{u_r}$$

$$\alpha = \omega_2/\omega_1 - 1, \quad x = \frac{r - r_1}{d}, \quad D = \frac{d}{dr}$$

$$Ta = 4\left(\frac{\omega_1 r_1^2 - \omega_2 r_2^2}{r_2^2 - r_1^2}\right)\frac{\omega_1 d^4}{\nu^2} = 2\left(\frac{V_1 d}{\nu}\right)^2\left(\frac{d}{r_1}\right)|_{\omega_2=0} \quad V_1 = \omega_1 r_1$$

TA = ratio centrifugal to viscous force

BC: $\widehat{u_r} = D\widehat{u_r} = u_\theta = 0 \quad x = 0{,}1$

The eigenvalues k at the marginal state are found by setting $\sigma = 0$ in the narrow gap equations subject the BC, as per Appendix B.

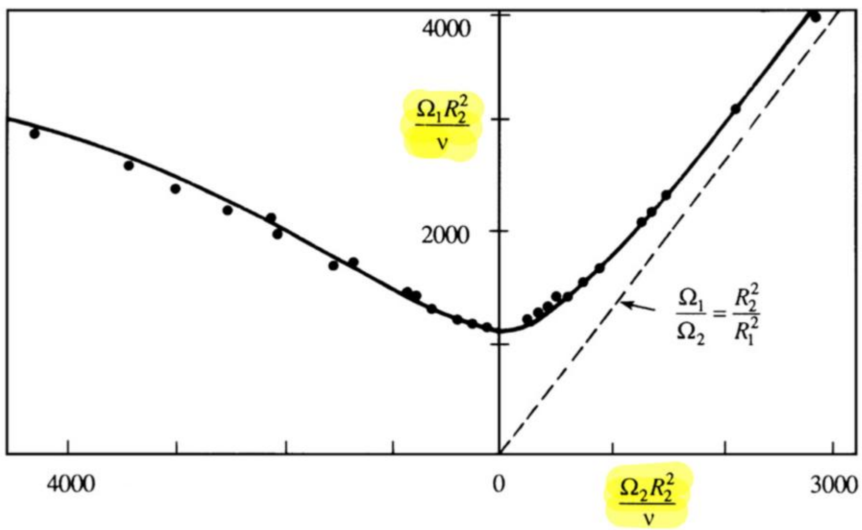

FIGURE 11.17 Taylor's observation and narrow-gap calculation of marginal stability in rotating Couette flow of water. The ratio of radii is $R_2/R_1 = 1.14$. The region above the curve is unstable. The dashed line represents Rayleigh's inviscid criterion, with the region to the left of the line representing instability. The experimental and theoretical results agree well and suggest that viscosity acts to stabilize the flow.

Solution small gap eigenvalue problem shows excellent agreement EFD

μ stabilizes the flow $\quad Ta_{critical} = \frac{1708}{(1/2)(1+\Omega_2/\Omega_1)}$

$k_{cr} = 3.12 \Rightarrow \lambda_{cr} = 2\pi d/k_{cr} = 2d$, i.e., height one cell $\approx d$ and vortices are square

At the time 1923 Taylor solution and EFD were considered confirmation NS and $\sigma_{ij} = -p\delta_{ij} + 2\mu\varepsilon_{ij}$

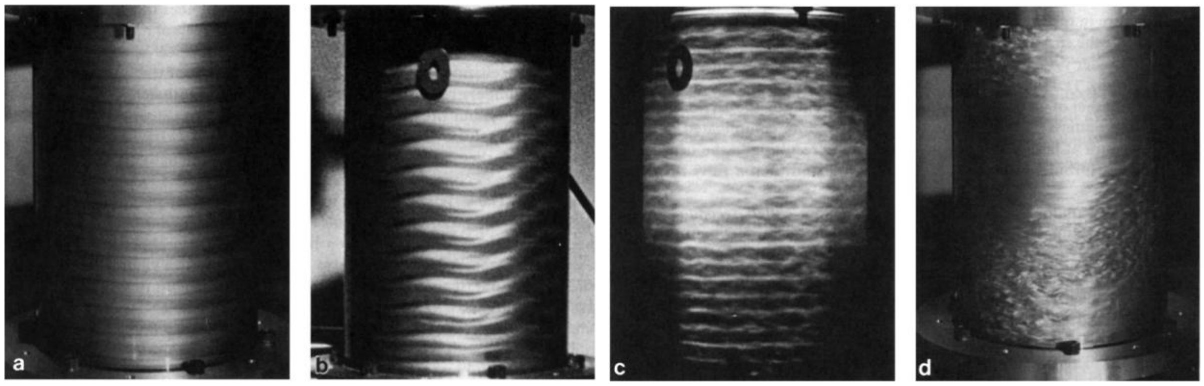

Taylor vortices for increasing Ta

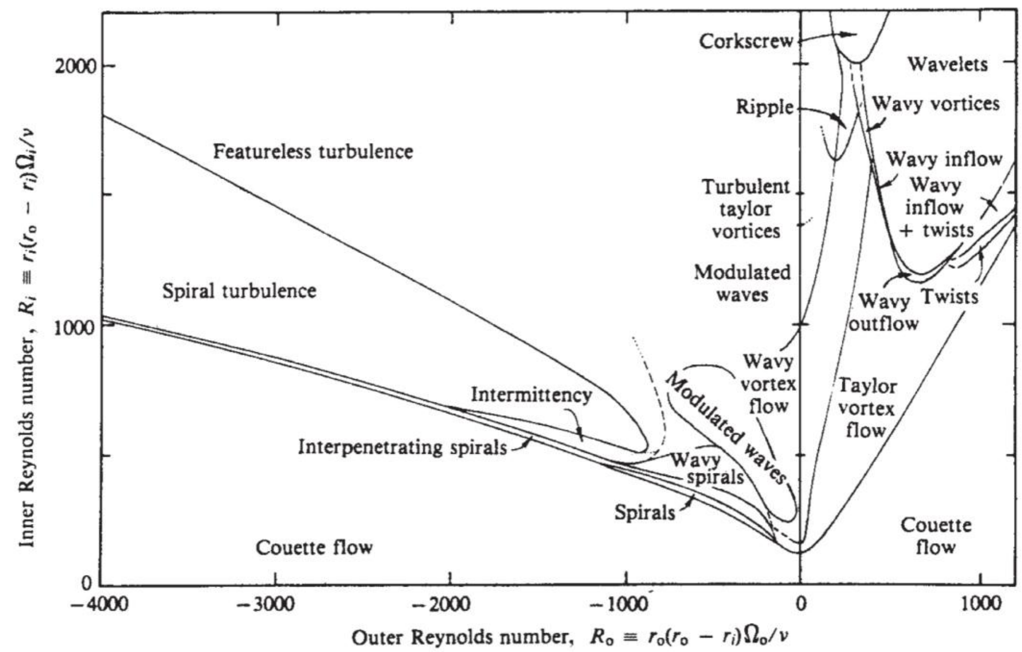

Figure 25.15 Stability chart for Taylor vortex behavior. Reprinted with permission from Andereck et al. (1986).